J|A|C|S
ARTICLES
Published on Web 01/26/2007

Fluorescent Pyrimidine Ribonucleotide: Synthesis, Enzymatic Incorporation, and Utilization

Seergazhi G. Srivatsan and Yitzhak Tor*

Contribution from the Department of Chemistry and Biochemistry, University of California, San Diego, La Jolla, California 92093-0358

Received September 6, 2006; E-mail: ytor@ucsd.edu

Abstract: Fluorescent nucleobase analogues that respond to changes in their microenvironment are valuable for studying RNA structure, dynamics, and recognition. The most commonly used fluorescent ribonucleoside is 2-aminopurine, a highly responsive purine analogue. Responsive isosteric fluorescent pyrimidine analogues are, however, rare. Appending five-membered aromatic heterocycles at the 5-position on a pyrimidine core has recently been found to provide a family of responsive fluorescent nucleoside analogues with emission in the visible range. To explore the potential utility of this chromophore for studying RNA−ligand interactions, an efficient incorporation method is necessary. Here we describe the synthesis of the furan-containing ribonucleoside and its triphosphate, as well as their basic photophysical characteristics. We demonstrate that T7 RNA polymerase accepts this fluorescent ribonucleoside triphosphate as a substrate in *in vitro* transcription reactions and very efficiently incorporates it into RNA oligonucleotides, generating fluorescent constructs. Furthermore, we utilize this triphosphate for the enzymatic preparation of a fluorescent bacterial A-site, an RNA construct of potential therapeutic utility. We show that the binding of this RNA target to aminoglycoside antibiotics, its cognate ligands, can be effectively monitored by fluorescence spectroscopy. These observations are significant since isosteric emissive U derivatives are scarce and the trivial synthesis and effective enzymatic incorporation of the furan-containing U triphosphate make it accessible to the biophysical community.

Introduction

Fluorescent nucleosides have become exceedingly instrumental in modern nucleic acids biophysics.[1] In particular, responsive nucleosides—chromophoric nucleobase analogues that respond to changes in their microenvironment via changes in their basic photophysical parameters—have found important applications in numerous bioanalytical and discovery assays.[1,2] To date, the most common fluorescent nucleoside to be utilized in exploring RNA recognition is 2-aminopurine (2-AP). A UV absorber and emitter (λ_{ex} 310, λ_{em} 370 nm, respectively), this adenosine mimic displays minimal emission when stacked with other bases, but upon unstacking and exposure to aqueous environments, a significantly enhanced emission is observed.[3,4] This useful reporting property has been elegantly exploited for studying RNA folding and recognition. Examples include "real-time" monitoring of the hammerhead ribozyme folding, cleavage and inhibition,[5] dimerization and isomerization of the HIV-1 dimerization initiation site,[6] RNA−protein interactions such as HIV RRE-Rev binding,[7] and, more recently, the binding of aminoglycoside antibiotics to the bacterial decoding site, known as the A-site.[8,9]

Remarkably, isosteric and functional fluorescent pyrimidine analogues are rare and, to the best of our knowledge, have not been extensively utilized in exploring RNA recognition pro-

(1) For review articles, see: (a) Millar, D. P. *Curr. Opin. Struct. Biol.* **1996**, *6*, 322−326. (b) Wojczewski, C.; Stolze, K.; Engels, J. W. *Synlett* **1999**, 1667−1678. (c) Hawkins, M. E. *Cell Biochem. Biophys.* **2001**, *34*, 257−281. (d) Murphy, C. J. *Adv. Photochem.* **2001**, *26*, 145−217. (e) Rist, M. J.; Marino, J. P. *Curr. Org. Chem.* **2002**, *6*, 775−793. (f) Okamoto, A.; Saito, Y.; Saito, I. J. *Photochem. Photobiol. C: Photochem. Rev.* **2005**, *6*, 108−122. (g) Ranasinghe, R. T.; Brown, T. *Chem. Commun.* **2005**, 5487−5502. (h) Silverman, A. P.; Kool, E. T. *Chem. Rev.* **2006**, *106*, 3775−3789. (i) Wilson, J. N.; Kool, E. T. *Org. Biomol. Chem.* **2006**, *4*, 4265−4274.

(2) Most efforts in developing fluorescent nucleosides have focused on DNA modifications. Selected examples include: (a) Coleman, R. S.; Madaras, M. L. *J. Org. Chem.* **1998**, *63*, 5700−5703. (b) Nakatani, K.; Dohno, C.; Saito, I. *J. Am. Chem. Soc.* **1999**, *121*, 10854−10855. (c) Seela, F.; Zulauf, M.; Sauer, M.; Deimel, M. *Helv. Chim. Acta* **2000**, *83*, 910−927. (d) Strässler, C.; Davis, N. E.; Kool, E. T. *Helv. Chim. Acta* **2000**, *83*, 2160−2171. (e) Hurley, D. J.; Seaman, S. E.; Mazura, J. C.; Tor, Y. *Org. Lett.* **2002**, *4*, 2305−2308. (f) Coleman, R. S.; Mortensen, M. A. *Tetrahedron Lett.* **2003**, *44*, 1215−1219. (g) Jiao, G.-S.; Kim, T. G.; Topp, M. R. Burgess, K. *Org. Lett.* **2004**, *6*, 1701−1704. (h) Okamoto, A.; Kanatani, K.; Saito, I. *J. Am. Chem. Soc.* **2004**, *126*, 4820−4827. (i) Dash, C.; Rausch, J. W.; Le Grice, S. F. J. *Nucleic Acids Res.* **2004**, *32*, 1539−1547. (j) Mayer, E.; Valis, L.; Wagner, C.; Rist, M.; Amann, N.; Wagenknecht, H.-A. *ChemBioChem* **2004**, *5*, 865−868. (k) Sandin, P.; Wilhelmsson, L. M.; Lincoln, P.; Powers, V. E. C.; Brown, T.; Albinsson, B. *Nucleic Acids Res.* **2005**, *33*, 5019−5025. (l) Okamoto, A.; Tainaka, K.; Nishiza, K.-I.; Saito, I. *J. Am. Chem. Soc.* **2005**, *127*, 13128−13129. (m) Okamoto, A.; Tainaka, K.; Saito, I. *Bioconjugate Chem.* **2005**, *16*, 1105−1111. (n) Gaballah, S. T.; Vaught, J. D.; Eaton, B. E.; Netzel, T. L. *J. Phys. Chem. B* **2005**, *109*, 5927−5934. (o) Andreatta, D.; Sen, S.; Perez, L. J. L.; Kovalenko, S. A.; Ernsting, N. P.; Murphy, C. J.; Coleman, R. S.; Berg, M. A. *J. Am. Chem. Soc.* **2006**, *128*, 6885−6892. (p) Kim, S. J.; Kool, E. T. *J. Am. Chem. Soc.* **2006**, *128*, 6164−6171. (q) Cho, Y.; Kool, E. T. *ChemBioChem* **2006**, *7*, 669−672.

(3) (a) Ward, D. C.; Reich, E.; Stryer, L. *J. Biol. Chem.* **1969**, *244*, 1228−1237. (b) Kawai, M.; Lee, M. J.; Evans, K. O.; Nordlund, T. M. *J. Fluorescence* **2001**, *11*, 23−32. (c) Jean, J. M.; Hall, K. B. *Proc. Natl. Acad. Sci. U.S.A.* **2001**, *98*, 37−41. (d) Rachofsky, E. L.; Osman, R.; Ross, J. B. A. *Biochemistry* **2001**, *40*, 946−956. (e) The 7-deaza and 8-aza-7-deaza analogues of 2-AP have been introduced. See: Seela, F.; Becher, G. *Helv. Chim. Acta* **2000**, *83*, 928−942.

(4) The quantum yield of the free 2-AP nucleoside in aqueous environment is 0.68 (ref 3d).

10.1021/ja066455r CCC: $37.00

cesses.[10,11] PyrroloC (pC), a recently introduced emissive C analogue, represents an exception. Similarly to 2-AP, pC is highly emissive as a free nucleoside and becomes progressively quenched upon introduction into a single-stranded RNA and RNA duplexes,[12] a property that has been utilized for monitoring RNA secondary structure.[13] To rectify this general deficiency in fluorescent pyrimidine analogues, we have recently initiated a program in the search for families of emissive and responsive nucleobase analogues. The basic requirements that are imposed upon the new nucleoside analogues include the following: (a) to maintain high structural similarity to the natural nucleobases; (b) to display emission at long wavelengths, preferably in the visible range; (c) to retain sufficient emission quantum efficiency to be utilized in real time fluorescence-based assays; and, importantly, (d) to possess sensitivity to the microenvironment that is manifested in markedly different photophysical parameters (emission wavelength λ_{em}, quantum efficiency ϕ_f and/or excited-state lifetime τ) in an aqueous versus apolar environment.

We have recently found and reported that appending five-membered aromatic heterocycles at the 5-position on a pyrimidine core generates a family of responsive fluorescent nucleoside analogues with emission in the visible range.[14] In particular, a 2′-deoxyuridine conjugated to a furan moiety was found to be very sensitive to changes in solvent environment, being fairly emissive in polar and rather nonemissive in apolar environments. When incorporated into DNA oligonucleotides and hybridized to complementary sequences, this furan analogue was found to positively signal the presence of DNA abasic sites, manifested via a 7-fold enhancement in emission of a "defective" DNA when compared to the emission of a perfect duplex.[14] We speculated that such responsive behavior could find use in exploring RNA recognition events, as these important biological processes typically involve intricate structural and dynamic changes that are likely to be translated into changes in the microenvironment of the participating reporter nucleotide. Here we describe the synthesis of the furan-containing ribonucleoside and its triphosphate, as well as their basic photophysical characteristics. We demonstrate that T7 RNA polymerase accepts this fluorescent ribonucleoside triphosphate as a substrate in *in vitro* transcription reactions and very efficiently incorporates it into RNA oligonucleotides.[15] Furthermore, we utilize this triphosphate for the enzymatic preparation of a fluorescent A-site construct. We show that the binding of this therapeutically important RNA target to aminoglycoside antibiotics, its cognate ligands, can be effectively monitored by fluorescence spectroscopy.

Scheme 1. Synthesis of Furan-Modified Nucleoside Triphosphate **2TP**[a]

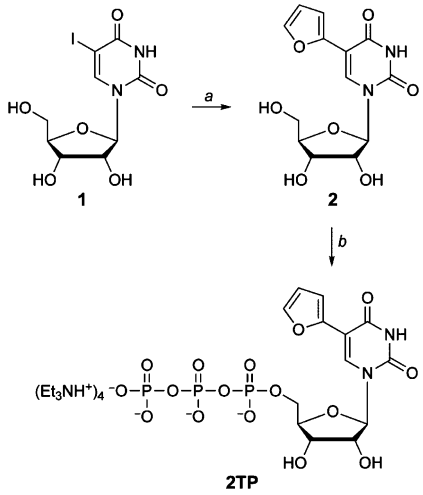

[a] Reagents and conditions: (a) 2-(Bu_3Sn)furan, $PdCl_2(PPh_3)_2$, dioxane, 90 °C, 98%. (b) (i) $POCl_3$, $(MeO)_3PO$, 0 °C; (ii) tributylammonium pyrophosphate, Bu_3N, 0 °C, 33%.

Results and Discussion

Synthesis and Photophysical Properties. Furan-modified ribonucleoside triphosphate **2TP**, necessary for transcription reactions, was synthesized in two steps (Scheme 1). Commercially available 5-iodouridine **1** was cross-coupled with 2-(tributylstannyl)furan in the presence of catalytic amounts of palladium to give the furan conjugated uridine **2**. Ribonucleoside **2** was then converted into the corresponding 5′-triphosphate **2TP** by a conventional method,[16] using freshly distilled $POCl_3$ and tributyl ammonium pyrophosphate. The triphosphate was extensively purified by ion exchange chromatography and HPLC and thoroughly characterized using mass spectrometry as well as, ^1H, ^{13}C and ^{31}P NMR spectroscopy (see Experimental Section).

The basic photophysical properties of the ribonucleoside **2** were evaluated prior to its incorporation into RNA oligonucleotides (Table 1). Ultraviolet spectra show two major absorption maxima at 254 and 316 nm, typical for the nucleoside and conjugated furan, respectively.[17] Increasing solvent polarity had little influence on the absorption maxima of the modified ribonucleoside, resulting in minor hypochromic and hyperchromic effects for the absorption maxima at 254 and 316 nm,

(5) (a) Menger, M.; Tuschl. T.; Eckstein, F.; Porschke, D. *Biochemistry* **1996**, *35*, 14710−14716. (b) Kirk, S. R.; Luedtke, N. W.; Tor, Y. *Bioorg. Med. Chem.* **2001**, *9*, 2295−2301.
(6) Rist, M. J.; Marino, J. P. *Nucleic Acids Res.* **2001**, *29*, 2401−2408.
(7) Lacourciere, K. A.; Stivers, J. T.; Marino, J. P. *Biochemistry* **2000**, *39*, 5630−5641. DeJong, E. S.; Chang, C. E.; Gilson, M. K.; Marino, J. P. *Biochemistry* **2003**, *42*, 8035−8046.
(8) Kaul, M.; Barbieri, C. M.; Pilch, D. S. *J. Am. Chem. Soc.* **2004**, *126*, 3447−3453.
(9) Shandrick, S.; Zhao, Q.; Han, Q.; Ayida, B. K.; Takahashi, M.; Winters, G. C.; Simonsen, K. B.; Vourloumis, D.; Hermann, T. *Angew. Chem., Int. Ed.* **2004**, *43*, 3177−3182.
(10) An isosteric fluorescent dC analogue has been reported: (a) Wut, P.; Nordlund, T. M.; Gildea, B.; McLaughlin, L. W. *Biochemistry* **1990**, *29*, 6508−6514. (b) Singleton, S. F.; Shan, F.; Kanan, M. W.; McIntosh, C. M.; Stearman, C. J.; Helm, J. S.; Webb, K. J. *Org. Lett.* **2001**, *3*, 3919−3922.
(11) For, site-specific fluorescent labeling of RNA molecules by transcription using unnatural base pairs, see: Kawai, R.; Kimoto, M.; Ikeda, S.; Mitsui, T.; Endo, M.; Yokoyama, S.; Hirao, I. *J. Am. Chem. Soc.* **2005**, *127*, 17286−17295. Endo, M.; Mitsui, T.; Okuni, T.; Kimoto, M.; Hirao, I.; Yokoyama, S. *Bioorg. Med. Chem. Lett.* **2004**, *14*, 2593−2596.
(12) To the best of our knowledge, the emission quantum yield for pyrroloC has not been rigorously determined (however, see: Liu, C.; Martin, C. T. *J. Mol. Biol.* **2001**, *308*, 465−475). Glen research reports quantum yield values of 0.07 and 0.02 for single- and double-stranded oligonucleotides, respectively.
(13) Tinsley, R.; Walter, N. G. *RNA* **2006**, *12*, 522−529.
(14) Greco, N. J.; Tor, Y. *J. Am. Chem. Soc.* **2005**, *127*, 10784−10785.
(15) Transcription using a nucleoside triphosphate was chosen as a method for incorporating the fluorescent nucleotide, because of the following: (a) simple synthesis − the triphospate is synthesized in two steps from commercially available precursors via procedures that do not require complicated protecting group chemistry necessary for solid-phase RNA synthesis; and (b) effective incorporation − reasonably large quantities of RNA can be synthesized by transcription reactions with relatively small amounts of the modified triphosphate. This makes the method accessible to almost all laboratories that are not necessarily equipped for complex organic synthesis and solid-phase RNA synthesis. It is important to note, however, that there is no inherent limitation for the synthesis of the corresponding phosphoramidite necessary for the solid-phase synthesis of modified RNA.
(16) Ludwig, J. *Acta Biochim. Biophys. Acad. Sci. Hung.* **1981**, *16*, 131−133.

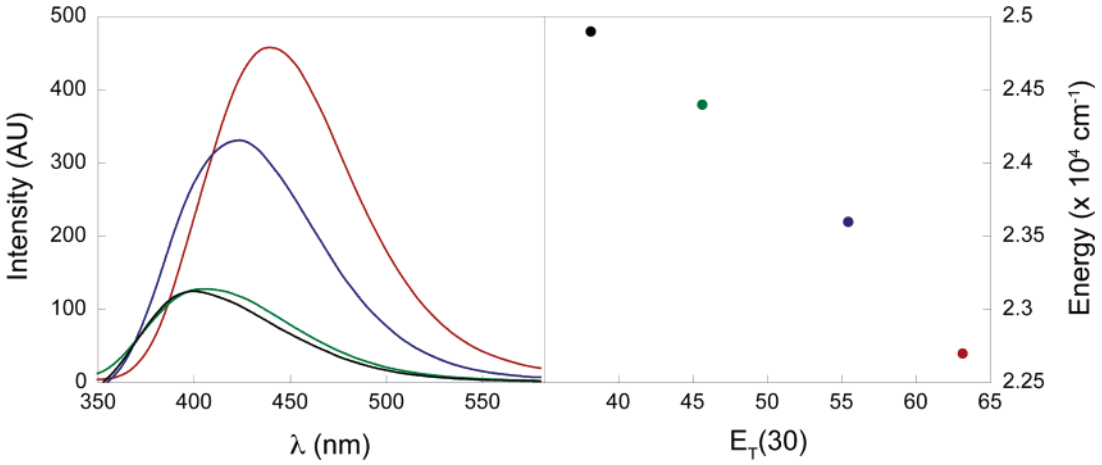

Figure 1. (Left) Emission spectra of nucleoside **2** (5.0×10^{-6} M) in water (red), methanol (blue), acetonitrile (green), and ethyl acetate (black). (Right) Emission energy plotted against $E_T(30)$, a microscopic solvent polarity scale.[18]

Table 1. Photophysical Data of Furan-Modified Uridine **2**[a]

solvent	λ_{max}[b] (nm)	λ_{em} (nm)	I_{rel}[c]
water	316	440	3.4
methanol	316	424	2.3
acetonitrile	314	410	1.0
ethyl acetate	314	401	1.0

[a] Conditions for absorption and emission spectra: 50 and 5.0×10^{-6} M, respectively. [b] The lowest energy maximum is given. Note the nucleoside shows another intense absorption at higher energies, around 250 nm; see Supporting Information for spectra. [c] Relative emission intensity with respect to intensity in ethyl acetate.

respectively (Figure S.1). When an aqueous solution of **2** was excited at 316 nm, a strong fluorescence emission at 440 nm was observed. The emission quantum yield for nucleoside **2**, determined relative to anthracene as standard, was found to be 0.035. In contrast to the ground state absorption profiles, the emission maximum (λ_{em}) and intensity were significantly affected by solvent polarity (Figure 1, Table 1). As solvent polarity was decreased from water to methanol, acetonitrile, and finally ethyl acetate, significant hypsochromic shift and hypochromic effects were observed. In water, **2** exhibited a strong emission band with the maximum at 440 nm corresponding to more than 3-fold higher intensity relative to its emission in ethyl acetate. An excellent correlation between emission energy and $E_T(30)$, a microscopic solvent polarity parameter,[18] is seen (Figure 1). A similar trend was previously reported for furan-modified thymidine under varying solvent polarity.[14,19] It is worth noting that the absorption and emission spectra of an aqueous solution of triphosphate **2TP** are essentially identical to those of the nucleoside **2** (Figures S.2 and S.3).

Enzymatic Incorporation of Furan-Modified U 2TP. *In vitro* transcription reactions in the presence of T7 RNA polymerase and triphosphate **2TP** were employed to investigate the enzymatic incorporation of the modified nucleotide into RNA oligonucleotides.[20] To evaluate the efficiency of transcription, an 18-mer T7 RNA polymerase consensus oligodeoxyribonucleotide promoter sequence was annealed to a synthetic DNA template **3a**. This template was designed to contain a unique deoxythymidine residue at the 5′-end.[21] When radiolabeled α-^{32}P ATP is used in the transcription reaction and the products are resolved on a denaturing sequencing polyacrylamide gel and visualized, full-length RNA transcripts are revealed via the formation of a radioactive band, while aborted transcripts remain undetected (Figure 2).

The annealed dsDNA was transcribed under standard *in vitro* transcription conditions in the presence of ATP, α-^{32}P ATP, GTP, CTP, and the furan-modified uridine triphosphate **2TP**. Phosphorimaging of the resolved transcription reaction shows the formation of a full length 10-mer RNA product along with trace amounts of $N + 1$ and $N + 2$ products with randomly incorporated noncoded extra bases, which is a common feature of such transcription reactions (Figure 3).[20] A control reaction in the absence of **2TP** did not result in the formation of any full-length product (Figure 3, lane 1). Taken together, these observations clearly indicate that the enzyme accepts and effectively incorporates the unnatural triphosphate **2TP** into the RNA strand. Performing the transcription reaction in the presence of increasing amounts of T7 RNA polymerase shows the optimal enzyme concentration under these conditions is 2.5 U/μL (Figure 3, lanes 2−4).

The transcription efficiency for the formation of the modified full-length product in the presence of **2TP** was found to be 78% relative to an unmodified RNA transcript, generated in the presence of UTP, the corresponding natural ribonucleoside triphosphate (Figure 4, lane 2).[22] Due to the incorporation of the higher MW furan-conjugated U, the modified RNA transcript compared to the unmodified transcript displayed a noticeable slower migration (Figure 4, compare lanes 1 and 2). The distinct migration of the two bands facilitates competition experiments between the modified triphosphate **2TP** and the parent UTP. Interestingly, transcription reactions performed with this template in the presence of equimolar concentrations of UTP and **2TP** illustrate that T7 RNA polymerase exhibits a slight preference for the modified triphosphate **2TP** over UTP with a ratio of 1.6:1 (Figure 4, lane 3).

(17) See Supporting Information for additional details.
(18) Reichardt, C. *Chem. Rev.* **1994**, *94*, 2319−2358.
(19) Slight differences between the absorption and emission of the deoxy furan containing nucleoside and its ribonucleoside counterpart are summarized in Table S.1. See Supporting Information.
(20) Milligan, J. F.; Uhlenbeck, O. C. *Methods Enzymol.* **1989**, *180*, 51−62.
(21) Tor, Y.; Dervan, P. B. *J. Am. Chem. Soc.* **1993**, *115*, 4461−4467.
(22) Transcription efficiencies are reported with respect to transcription in the presence of natural nucleotides and represent the average of two independent reactions. Errors are ±10%; see Experimental Section.

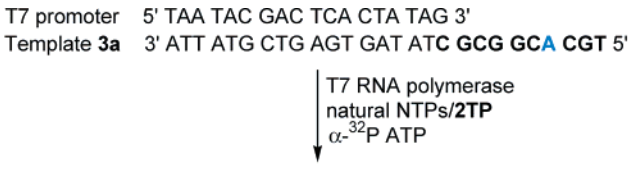

DNA templates	Transcripts
3a 3' ATT ATG CTG AGT GAT ATC GCG GCA CGT 5'	**4a** 5' pppGCG CCG UGC A 3'
3b 3' ATT ATG CTG AGT GAT ATC ACG GCG CGT 5'	**4b** 5' pppGUG CCG CGC A 3'
3c 3' ATT ATG CTG AGT GAT ATC GAG GCC CGT 5'	**4c** 5' pppGCU CCG GGC A 3'
3d 3' ATT ATG CTG AGT GAT ATC GCA GCG CGT 5'	**4d** 5' pppGCG UCG CGC A 3'
3e 3' ATT ATG CTG AGT GAT ATC GCA GCA CGT 5'	**4e** 5' pppGCG UCG UGC A 3'
3f 3' ATT ATG CTG AGT GAT ATC GCG GAA CGT 5'	**4f** 5' pppGCG CCU UGC A 3'

Figure 2. Enzymatic incorporation of furan-modified ribonucleotide triphosphate **2TP**. DNA templates **3a**−**3f** annealed to 18-mer consensus T7 promoter and corresponding RNA transcripts **4a**−**4f**. Modified bases in the transcripts are highlighted in red.

Figure 3. Transcription reactions with template **3a** in the presence of furan-modified **2TP** and varying concentrations of T7 RNA polymerase. Lane 1: Control reaction in the absence of **2TP**. Lanes 2−4: T7 RNA polymerase concentrations: 1, 2, and 2.5 U/μL, respectively.

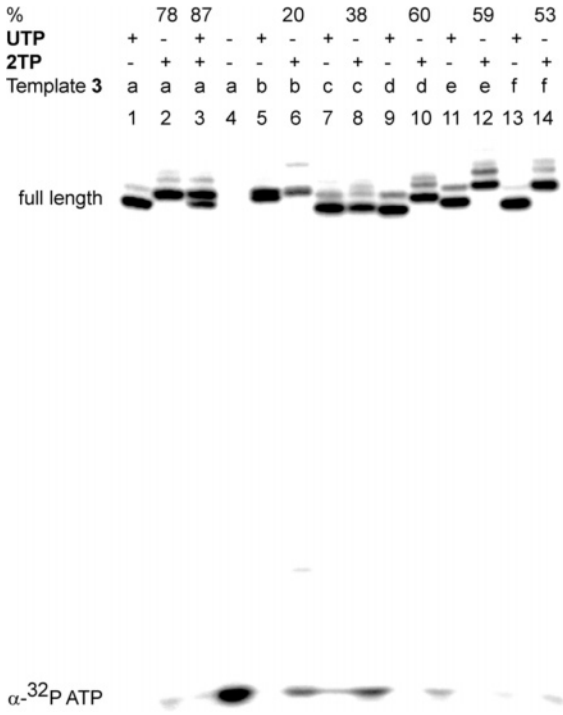

Figure 4. Transcription reaction to study the incorporation efficiency of **2TP** at various positions in the transcript using different templates. Percent incorporation of **2TP** is reported with respect to transcription in the presence of UTP.

Transcription reactions are known to be susceptible to the sequence of the DNA template, particularly near the promoter region.[20] Transcription efficiency is greatly reduced when the +1 or +2 guanosine bases proximal to the promoter sequence are replaced with other nucleotides, while the enzyme tends to better tolerate changes in +3 to +6 bases with little effect on the transcription yield.[20,23] To evaluate the potential of the enzyme to incorporate the modified uridine closer to the promoter region, we designed templates, which would lead to the incorporation of **2TP** in position +2 to +7 (Figure 2). In the presence of template **3b**, a modified base is added at +2 position with 20% efficiency (Figure 4, lane 6). The extent of transcription substantially improved in the case of template **3c** and **3d** resulting in the substitution at +3 and +4 (Figure 4, lane 8, 10). Importantly, we were also able to doubly modify RNA transcripts with both spaced and adjacent modified uridines in reasonable yields using templates **3e** (59%) and **3f** (53%), respectively (Figure 4, lane 12, 14).

Characterization of the RNA Transcript. To further establish the presence of the furan modification in the transcription product, large-scale transcription reactions with template **3a** using non-radiolabeled triphosphates were performed (see Experimental Section). Gel electrophoretic purification of the reaction mixture afforded nearly 14 nmol of the RNA product with approximately 200-fold amplification over the amount of the DNA template. To determine its composition, the transcript was subjected to enzymatic digestion in the presence of alkaline phosphatase, phosphodiesterase, RNase A, and RNase T1, and the digest was analyzed by reversed-phase HPLC.[24] The HPLC profile clearly shows the presence of nucleoside **2** in the digest (Figure 5). The nucleoside composition (G/C/A/**2** = 4.10:4.05:1.00:1.02) matched well with the expected full length RNA sequence (Figure 2). Fractions corresponding to the retention times of each nucleoside were collected from the HPLC run, and subsequent mass spectral analysis further confirmed the

(23) Milligan, J. F.; Groebe, D. R.; Witherell, G. W.; Uhlenbeck, O. C. *Nucleic Acids Res.* **1987**, *15*, 8783−8798.
(24) Buck, M.; Connick, M.; Ames, B. N. *Anal. Biochem.* **1983**, *129*, 1−13.

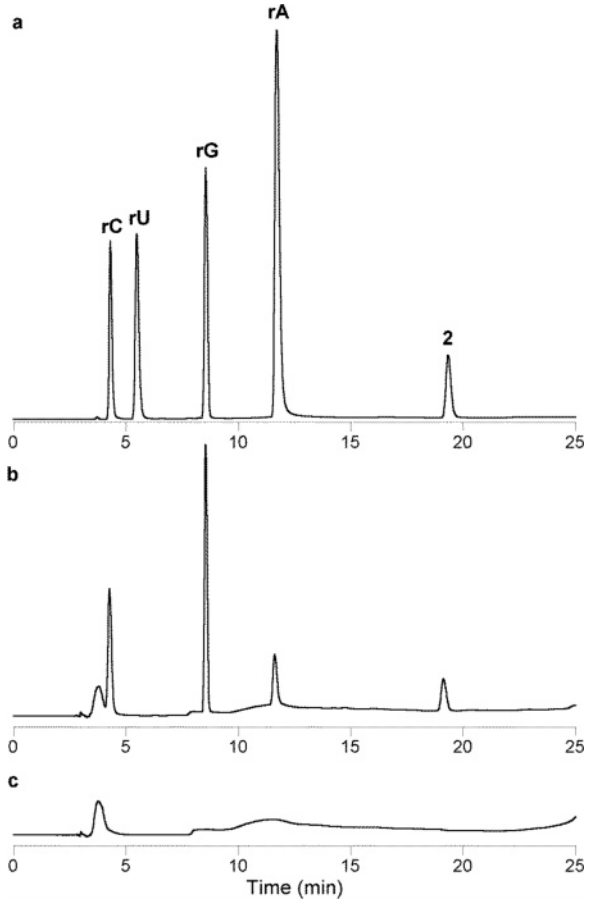

Figure 5. HPLC profile of enzymatic digestion of transcript at 260 nm. (a) Authentic nucleoside samples and modified nucleoside **2**. (b) Digested RNA transcript. (c) Control digestion reaction in the absence of RNA transcript. See Experimental Section for conditions.

authenticity of the native and modified nucleosides. Moreover, MALDI-TOF MS measurement of the transcript also established the incorporation of **2** in the full-length transcript (Figure 6). These results unambiguously demonstrate the incorporation of fluorescent furan-modified U analogue **2** into the RNA strand by *in vitro* transcription reactions.

An aqueous solution of the RNA transcript **4a** shows, in addition to a strong absorption of the native nucleotides around 260 nm, absorption at longer wavelengths (λ_{max} 322 nm), slightly red-shifted when compared to the free nucleoside (λ_{max} 316 nm) (Figure S.2). The fluorescence spectrum of this RNA transcript shows an intense emission at 437 nm, similar to the emission profile of the free nucleoside **2** in water (λ_{em} 440 nm), suggesting the modified nucleobase, within this single-stranded RNA, is residing in a rather polar microenvironment (Figure S.3). Importantly, the emission intensity of the RNA transcript is about 3-fold lower than that of the free nucleoside or its triphosphate, suggesting partial stacking of the chromophore or quenching by neighboring nucleobases (Figure S.3, S.4).[25,26]

(25) Note this trend (i.e., significantly quenched emission in oligonucleotides when compared to the free nucleoside) is not unique to chromophore **2**. 2-AP and pC both qualitatively show similar behaviors, where the incorporated nucleoside when compared to the free nucleoside in aqueous solution is much less emissive. Extensive studies with 2-AP-containing oligonucleotides have suggested that both base stacking and collisions with neighboring bases contribute to quenching. See ref 3d.

(26) See Supporting Information for preliminary Stern−Volmer titrations of **2** with all four native nucleotide monophosphates (Figure S.4).

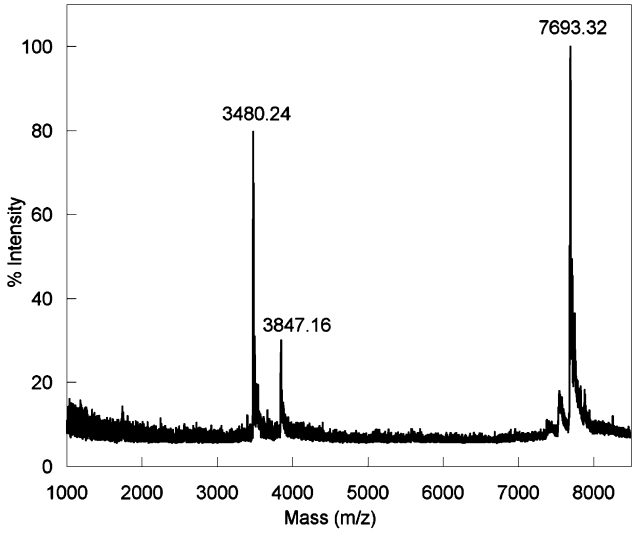

Figure 6. MALDI-TOF MS spectrum of furan-labeled RNA transcript calibrated relative to the +1 and +2 ions of an internal 25-mer DNA standard (*m*/*z*: 7693.32 and 3847.16). Calculated mass [M] = 3479.39; observed mass = 3480.24.

Assay Development: General Considerations. Several concerns have to be addressed when a fluorescently labeled RNA sequence is enzymatically synthesized. Ideally, one would like to implant the reporter nucleotide close to the recognition site without altering the recognition properties. In this particular case, utilizing "isomorphic" fluorescent nucleobases has certain advantages, as minor structural perturbations are likely to be well-tolerated and modified targets of comparable recognition features are likely to be generated. The nature of the transcription reaction itself imposes, however, certain practical restrictions on the implementation of this approach. A priori, two extreme labeling procedures can be considered: (a) substitution of all native residues with the corresponding modified fluorescent analogue (e.g., all U residues for **2**) and (b) a sequence-specific modification of a unique, strategically placed residue. While the former approach is the easiest to implement experimentally, it is unlikely to provide a general solution. The two major disadvantages of the "total labeling" approach include the following: (a) a potentially more severe structural perturbation of the RNA target, and (b) a probable poor photophysical performance due to the presence of multiple chromophores with potentially canceling effects, resulting in relatively weak signal changes induced upon ligand binding. On the other hand, sequence specific substitution of a single residue with an environmentally sensitive fluorescent nucleotide is likely to result in favorable photophysical characteristics of the RNA construct. The challenge associated with this approach, however, is the design of the RNA constructs to allow for the enzymatic incorporation of a single modified residue.

To explore the potential utility of the furan-modified uridine **2TP** for the investigation of RNA−ligand interactions, we have selected the bacterial decoding A-site as a test system. This RNA sequence has been vigorously investigated in recent years as a potential therapeutic target for the development of new antibiotics.[27] The A-site provides an opportunity to face the challenges discussed above and scrutinize the technical aspects

(27) Hermann, T.; Tor, Y. *Expert Opin. Ther. Pat.* **2005**, *15*, 49−62.

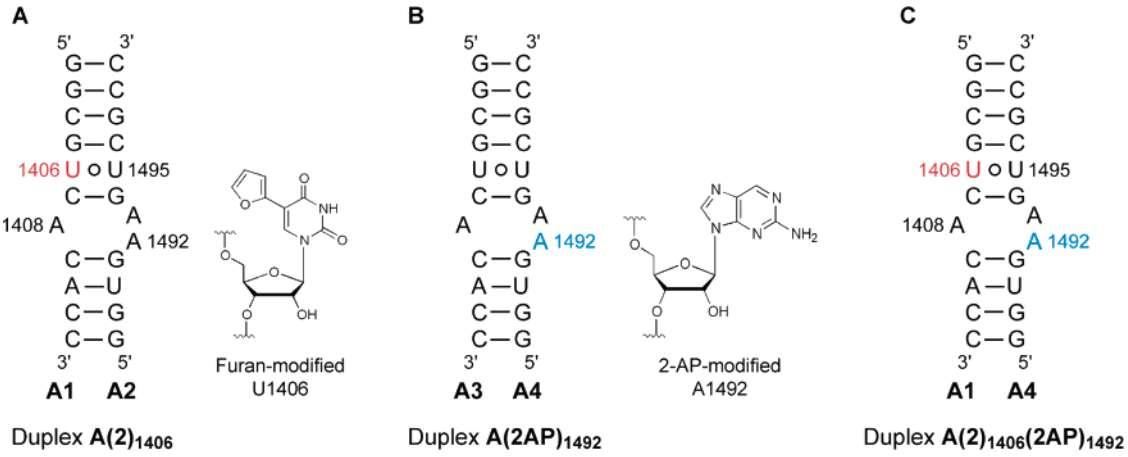

Figure 7. (A) Secondary structure of furan-labeled A-site duplex model **A(2)$_{1406}$** used in this study and structure of fluorescent label at U1406 are shown. (B) Secondary structure of 2-AP-labeled A-site duplex model **A(2AP)$_{1492}$** used in this study and structure of 2-AP label at A1492 are shown. (C) A hybrid A-site duplex containing the furan-modified U at position 1406 and 2-AP at position 1492.

involved in enzymatically labeling an RNA target of true biological and medicinal chemistry significance.

Binding of Aminoglycoside Ligands to Fluorescently Labeled A-Site. New antibiotics are required to complement and ultimately replace the currently available drugs that are increasingly being compromised by the evolvement of resistant strains.[28] One of the key targets for antibiotics is the bacterial ribosome.[29] Screening approaches for ribosome-targeted antibacterials have traditionally relied on time-consuming functional assays that probe the interference of compounds with *in vitro* translation assays or the inhibition of bacterial growth. Progress in the structural determination of RNA domains and their complexes with small molecules[30,31] is now paving the way for more rational drug discovery approaches focusing on the bacterial ribosomal RNA as a target.[32] The decoding, or A-site, a small internal loop within the 16S rRNA, is the molecular target for the naturally occurring aminoglycoside antibiotics.[33] Biochemical and structural studies have demonstrated that this site is an autonomous RNA domain capable of mimicking the function and recognition features of the entire 16S rRNA.[34] This important correlation has paved the way for the development of useful fluorescence-based assays for the discovery of A-site binders utilizing short RNA constructs.[8,9,35]

Aminoglycoside antibiotics interfere with the conformational flexibility of two adenine residues, A1492 and A1493, that are involved in mRNA decoding (Figure 7). Recent structural investigations indicate that aminoglycosides form direct hydrogen bonds to the Watson−Crick sites of A1408 and subsequently bulge out A1492 and A1493 from the helix.[36] Substituting any of these dynamic purine residues with 2-AP has been shown to generate fluorescent RNA constructs, which faithfully report on aminoglycoside binding and therefore constitute useful binding assays.[8,9] Additional direct or water-bridged H-bonds to the neighboring G−C pairs and the noncanonical U1406oU1495 pair further stabilize the A-site−aminoglycoside complexes and prompt us to consider replacing one of the U residues with a fluorescent furan-containing analogue **2** as a means for generating a fluorescent reporting A-site construct.

To avoid multiple modifications during the enzymatic synthesis of the modified A-site, a duplex construct, which fundamentally represents the binding site of aminoglycosides to the wild type, was employed (Figure 7). RNA strand **A1** contains only one uridine residue (1406) and, hence, can be selectively labeled using T7 RNA polymerase. A transcription reaction was performed in the presence of **2TP**, and the transcript was purified by gel electrophoresis. MALDI-TOF mass measurement confirmed the presence of the modified full-length product **A1** (Figure S.7). A 1:1 mixture of modified RNA strand **A1** and the synthetic counterstrand **A2** was hybridized in HEPES buffer pH 7.4 (see Figure S.5 for thermal denaturation experiments).[37] The resulting labeled A-site duplex **A(2)$_{1406}$** (4.0 μM) was excited at 322 nm, and changes in emission upon titration with aminoglycosides were monitored at 433 nm. As seen in Figure 8, titration of paromomycin to **A(2)$_{1406}$** resulted in nearly a 2-fold increase in emission intensity corresponding to an EC_{50} value of 11.5 ± 0.9 μM.[38] As a control, titration of the single-stranded **A1** with paromomycin shows much smaller changes in emission (Figure 8B).[39]

To draw parallels with the reported 2-AP-based assays, we constructed an A-site duplex model, where an unmodified transcript **A3** was annealed to an RNA strand **A4**, containing a 2-AP at position 1492 (Figure 7). The resulting duplex **A-**

(28) (a) Neu, H. C. *Science* **1992**, *257*, 1064−1073. (b) Kotra, L. P.; Haddad, J.; Mobashery, S. *Antimicrob. Agents Chemother.* **2000**, *44*, 3249−3256. (c) Jansen, W. T. M.; van der Bruggen, J. T.; Verhoef, J.; Fluit, A. C. *Drug Resist. Updates* **2006**, *9*, 123−133.
(29) Knowles, D. J.; Foloppe, N.; Matassova, N. B.; Murchie, A. I. *Curr. Opin. Pharmacol.* **2002**, *2*, 501−506.
(30) (a) Fourmy, D.; Recht, M. I.; Blanchard, S. C.; Puglisi, J. D. *Science* **1996**, *274*, 1367−1371. (b) Yoshizawa, S.; Fourmy, D.; Puglisi, J. D. *EMBO J.* **1998**, *17*, 6437−6448.
(31) (a) Vicens, Q.; Westhof, E. *Structure* **2001**, *9*, 647−658. (b) Vicens, Q.; Westhof, E. *Chem. Biol.* **2002**, *9*, 747−755.
(32) (a) Chow, C. S.; Bogdan, F. M. *Chem. Rev.* **1997**, *97*, 1489−1513. (b) Tor, Y. *Angew. Chem., Int. Ed.* **1999**, *38*, 1579−1582. (c) Hermann, T. *Angew. Chem., Int. Ed.* **2000**, *39*, 1890−1905. (d) Hermann, T.; Patel, D. J. *Science* **2000**, *287*, 820−825. (e) Sucheck, S. J.; Wong, C.-H. *Curr. Opin. Chem. Biol.* **2000**, *4*, 678−686. (f) Wilson, W. D.; Li, K. *Curr. Med. Chem.* **2000**, *7*, 73−98. (g) Gallego, J.; Varani, G. *Acc. Chem. Res.* **2001**, *34*, 836−843. (h) Tor, Y. *Chem. Biol. Chem.* **2003**, *4*, 998−1007.
(33) Moazed, D.; Noller, H. F. *Nature* **1987**, *327*, 389−394.
(34) Purohit, P.; Stern, S. *Nature* **1994**, *370*, 659−662.
(35) For an A-site construct labeled at its terminus with fluorescein, see: Haddad, J.; Kotra, L. P.; Llano-Sotelo, B.; Kim, C.; Azucena, E. F., Jr.; Liu, M.; Vakulenko, S. B.; Chow, C. S.; Mobashery, S. *J. Am. Chem. Soc.* **2002**, *124*, 3229−3237.
(36) Francois, B.; Russell, R. J. M.; Murray, J. B.; Aboul-ela, F.; Masquida, B.; Vicens, Q.; Westhof, E. *Nucleic Acids Res.* **2005**, *33*, 5677−5690.
(37) Thermal denaturation studies with singly modified RNA duplexes show no detrimental effect on the furan modification on duplex stability. See Figures S.5 and S.6 in the Supporting Information for data.
(38) EC_{50} is the concentration required for 50% response.

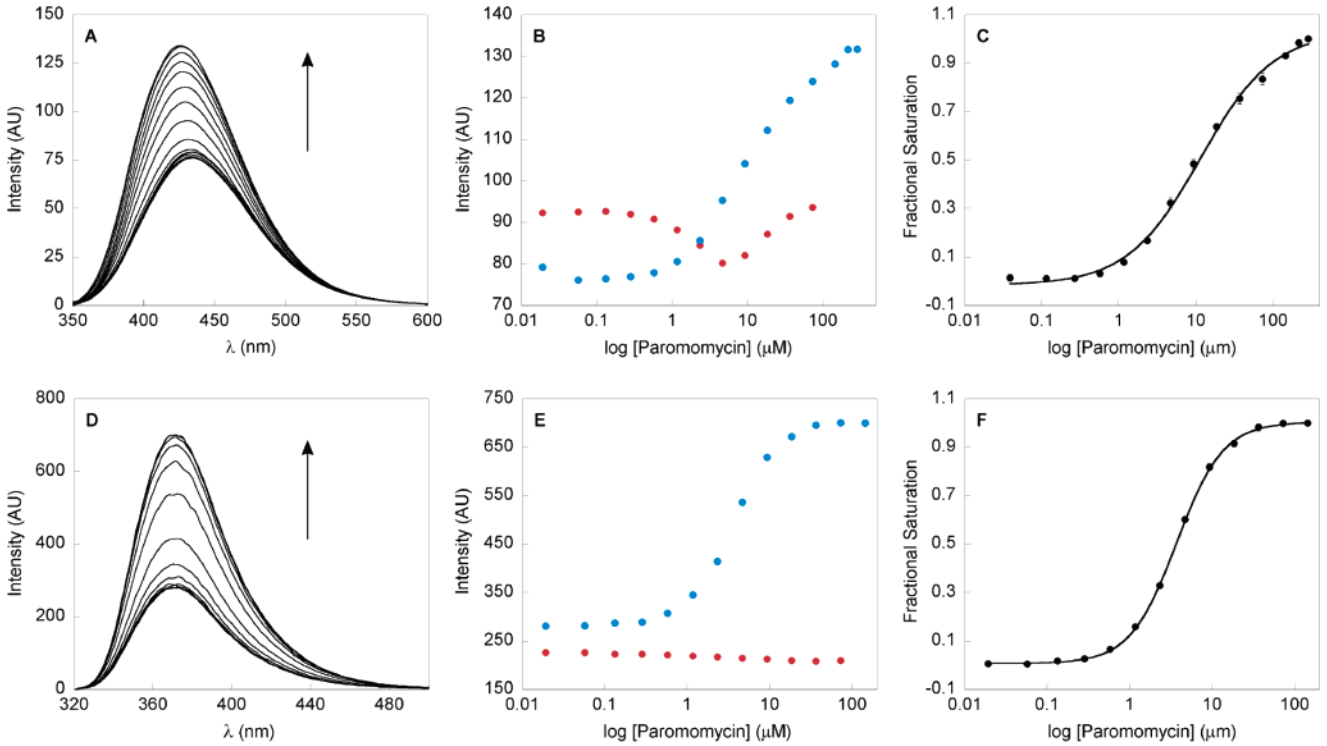

Figure 8. Fluorescence titrations of A-site constructs with paromomycin. Titrations were performed in HEPES buffer (pH 7.4) containing 4.0 μM RNA (see Experimental Section for details). Top: (A) Representative emission spectra for the titration of A-site duplex **A(2)$_{1406}$** with paromomycin, where fluorescence intensity increases with increasing concentrations of aminoglycoside. (B) Fluorescence intensity is plotted against log of paromomycin concentration: ssRNA, **A1** (red) and duplex, **A(2)$_{1406}$** (blue). (C) Curve fit for the titration of duplex **A(2)$_{1406}$** with aminoglycoside. Bottom: (D) Representative emission spectra for the titration of A-site duplex **A(2AP)$_{1492}$** with paromomycin, where fluorescence intensity increased with increasing concentrations of aminoglycoside. (E) Fluorescence intensity is plotted against log of paromomycin concentration: ssRNA, **A4** (red) and duplex, **A(2AP)$_{1492}$** (blue). (F) Curve fit for the titration of duplex **A(2AP)$_{1492}$** with aminoglycoside. See Experimental Section for conditions.

(2AP)$_{1492}$ was excited at 310 nm, and conformational changes incurred upon paromomycin binding were monitored at the emission maximum of 2-AP (371 nm) (Figure 8D−F). Much like previous studies, titrations performed under similar conditions led to a significant increase in fluorescence intensity, displaying a comparable EC_{50} value (3.7 ± 0.03 μM) (Figure 8F).[40] Literature precedence suggests that binding of paromomycin to the decoding site flips out and unstacks the nucleotide 1492, resulting in enhanced 2-AP fluorescence.[9] Control titrations carried out by adding paromomycin to 2-AP-modified **A4** single-stranded RNA showed no significant change in fluorescence (Figure 8E).[39]

The slight discrepancy in EC_{50} values obtained with duplex **A(2)$_{1406}$** and **A(2AP)$_{1492}$** can, in principle, be attributed to the relative affinity of paromomycin to these modified duplexes. X-ray crystallographic data indicate that the introduction of the 2-AP label does not significantly alter the interaction of aminoglycosides with the target RNA.[9] In the absence of structural analysis of modified A-site **A(2)$_{1406}$**,[41] we speculate that conjugating a furan to U1406 might slightly alter the binding pockets where the antibiotics reside. Published crystal structures of aminoglycoside−A-site complexes show water-mediated interactions between the U1495•U1406 pair.[32,36] Placement of the hydrophobic furan ring in proximity to this pocket may alter hydration and slightly diminish these secondary interactions.

Neomycin binding to A-site constructs was also investigated. Binding of neomycin to furan-modified duplex **A(2)$_{1406}$** was signaled by enhanced fluorescence corresponding to an EC_{50} value of 5.02 ± 0.24 μM (Figure 9). The higher affinity exhibited by neomycin for the A-site as compared to paromomycin is in agreement with other literature reports.[40c,42] Interestingly, 2-AP-modified duplex **A(2AP)$_{1492}$** failed to show any significant response to neomycin titration.[43]

In principle, two different fluorophores can be simultaneously incorporated into an RNA duplex and, ideally, independently

(39) In certain cases the single-stranded control sequences respond to increasing concentrations of aminoglycosides. Examination of the single-stranded oligonucleotides **A1** and **A4** shows that they can form a "self-complementary" metastable duplex with eight base pairs and three noncanonical (likely bulged out) A•C and C•C "pairs" (see Figure S.8 in the Supporting Information). The single-stranded oligonucleotide is therefore likely to provide a target for positively charged aminoglycosides, as these antibiotics are known to bind numerous RNA structures in a nonspecific fashion through electrostatic interactions (see ref 33h and Zhao, F.; Zhao, Q.; Blount, K. F.; Han, Q.; Tor, Y.; Hermann, T. *Angew. Chem., Int. Ed.* **2005**, *44*, 5329−5334). It is also important to note that the 2-AP-containing single strand, although not apparent from Figures 8E and 9E, is also responding to increasing paromomycin and neomycin concentrations (see Figures S.9 and S.10 in the Supporting Information plotted using an expanded scale).

(40) (a) Lynch, S. R.; Puglisi, J. D. *J. Mol. Biol.* **2001**, *306*, 1037−1058. (b) Griffey, R. H.; Hofstalder, S. A.; Sannes-Lowery, K. A.; Ecker, D. J.; Crooke, S. T. *Proc. Natl. Acad. Sci. U.S.A.* **1999**, *96*, 10129−10113. (c) Wong, C. H.; Hendrix, M.; Priestley, E. S.; Greenberg, W. A. *Chem. Biol.* **1998**, *5*, 397−406. (d) Recht, M. I.; Fourmy, D.; Blanchard, S. C.; Dahlquist, K. D.; Puglisi, J. D. *J. Mol. Biol.* **1996**, *262*, 421−436.

(41) Crystallization of the furan-modified RNA constructs with and without aminoglycosides is in progress.

(42) (a) Pilch, D. S.; Kaul, M.; Barbieri, C. M.; Kerrigan, J. E. *Biopolymers* **2003**, *70*, 58−79. (b) Ryu, D. H.; Rando, R. R. *Bioorg. Med. Chem.* **2001**, *9*, 2601−2608.

(43) Neomycin B is known to present challenges for 2-AP-labeled A-site constructs. Fluorescent detection can be observed under modified ionic strength conditions, but even then the fluorescence response is significantly weaker than that induced by paromomycin (D. Pilch and T. Hermann, personal communications). Although crystal structures of neomycin and paromomycin complexed with the A-site nearly superimpose each other, at this point there is no satisfactory explanation for the inability of 2-AP model constructs to effectively report on neomycin binding.

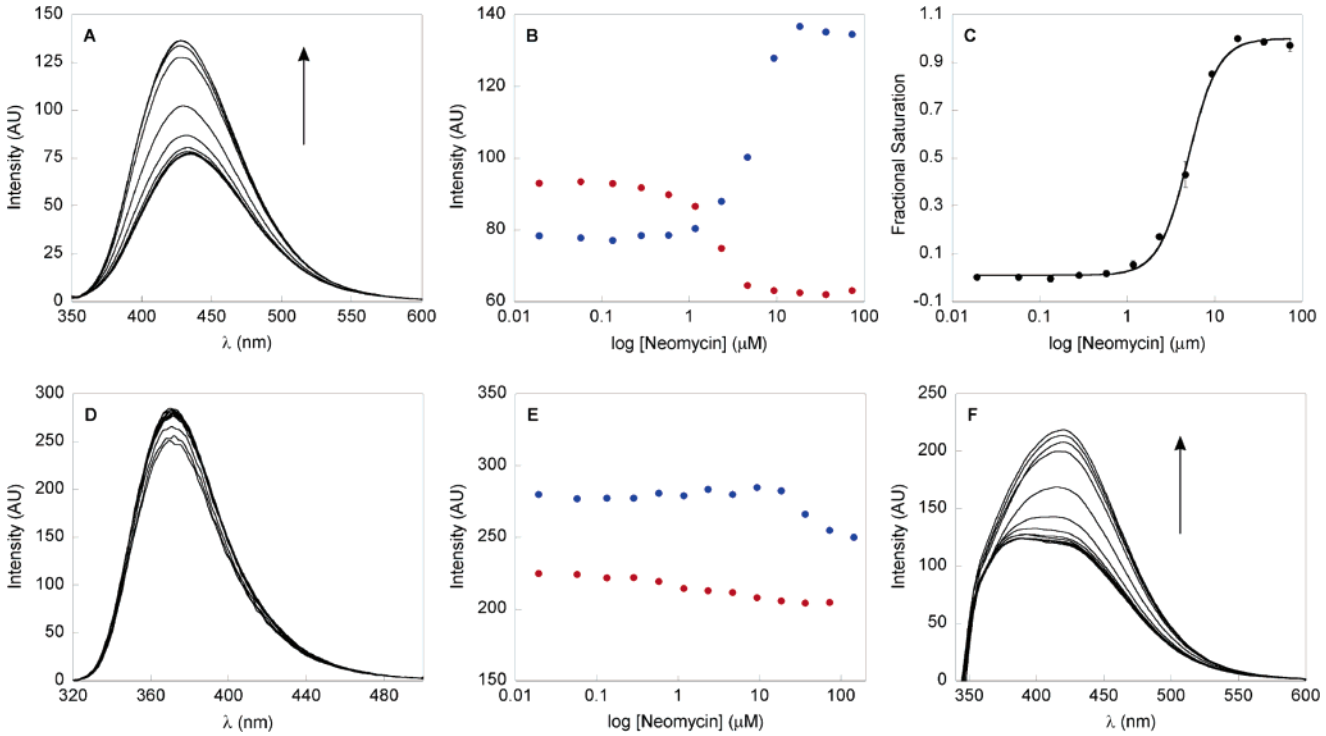

Figure 9. Top: Binding isotherms for the fluorescence titration of furan-labeled ssRNA (**A1**), duplex $\mathbf{A(2)_{1406}}$ with neomycin. (A) Representative emission spectra for the titration of duplex $\mathbf{A(2)_{1406}}$ with neomycin, where fluorescence intensity increased with increasing concentrations of aminoglycoside. (B) Fluorescence intensity is plotted against log of neomycin concentration: ssRNA, **A1** (red) and duplex, $\mathbf{A(2)_{1406}}$ (blue). (C) Curve fit for the titration of duplex $\mathbf{A(2)_{1406}}$ with neomycin. Bottom: (D) Emission spectra for the titration of 2-AP-labeled duplex $\mathbf{A(2AP)_{1492}}$ with neomycin. (E) Fluorescence intensity is plotted against log of neomycin concentration: ssRNA, **A4** (red) and duplex, $\mathbf{A(2AP)_{1492}}$ (blue). In both of the RNA constructs no significant change in fluorescence was observed.[39] (F) Fluorescence emission spectra for the titration of A-site duplex $\mathbf{A(2)_{1406}(2AP)_{1492}}$ derived from furan-labeled **A1** and 2-AP-labeled **A4** RNA with neomycin. The duplex was excited at 335 nm to obtain comparable emission for both fluorophores. Fluorescence intensity increased with increasing concentrations of neomycin, corresponding to the emission maximum of the furan conjugate. Note the minimal response of 2-AP under these conditions.

monitored. Such a dual-emitting system requires chromophores with overlapping excitation wavelengths but well separated emission maxima. 2-AP and the furan-modified nucleoside **2** fulfill this criteria to a certain degree, with typical excitation wavelengths of 310 and 322 nm, respectively. Since the furan-modified nucleoside **2** has, however, a much larger Stokes' shift, the emission lines are appreciably separated (emission at ~370 and ~430 nm for 2-AP and **2**, respectively). A hybrid duplex $\mathbf{A(2)_{1406}(2AP)_{1492}}$ was therefore assembled and used to further probe the binding of neomycin B to these fluorescent A-site constructs. Since 2AP has, however, a higher quantum yield than **2**, the hydrid RNA duplex $\mathbf{A(2)_{1406}(2AP)_{1492}}$ was excited at a common wavelength (335 nm) to obtain comparable initial fluorescence for both fluorophores (Figure 9F). When titrated with neomycin, the A-site duplex $\mathbf{A(2)_{1406}(2AP)_{1492}}$ effectively indicates a binding event with enhanced fluorescence corresponding to the emission characteristic of furan-modified **2** at 433 nm (Figure 9F), with a minimal response of 2-AP.[44] This experiment suggests that 2-AP incorporation at 1492 does not hamper neomycin from binding to this A-site duplex model. Furan-modified U **2** provides, therefore, a useful fluorescent probe for the detection of neomycin binding, a process that, in this particular case, cannot be effectively monitored using 2-AP, the most common fluorescent probe to be utilized for RNA−ligand interactions.

Summary and Implications

To explore the potential utility of new chromophores for studying RNA−ligand interactions, the enzymatic incorporation of a furan-modified ribonucleotide **2TP** was examined. T7 RNA polymerase accepts this fluorescent ribonucleoside triphosphate as a substrate and very effectively incorporates it into RNA oligonucleotides. The resulting fluorescent RNA constructs can be prepared in large scale and utilized for exploring RNA recognition events. In particular, we demonstrate that a fluorescent bacterial A-site can be effectively labeled and productively examined using fluorescent spectroscopy. We show that the binding of this RNA target to aminoglycoside antibiotics, its cognate ligands, can be effectively monitored by changes in the fluorescence intensity of the probe.

Our studies highlight the scope and the general limitations associated with the utilization of fluorescent nucleobases for the study of nucleic acids−ligand interactions. Comparative studies with RNA constructs labeled with 2-AP, the most commonly used responsive fluorescent ribonucleoside, illustrate the lack of a general solution to this important task. The use of a "universal" fluorescent probe is unlikely to be realistic. Multiple constructs and, if possible, multiple probes should be examined. Differences in probe behavior can, in principle, be attributed to various effects, not all apparent from the sequence itself. In particular, different interactions with neighboring bases in the free and bound state can lead to a relatively weak overall photophysical response even if binding affinity itself is unaffected. This highlights the challenges associated with the application of fluorescent nucleobases and the need for the

(44) Note, however, that when duplex $\mathbf{A(2)_{1406}(2AP)_{1492}}$ is titrated with parmomycin, both fluorophores respond. See Figure S.12 in the Supporting Information.

design and synthesis of new and complementary fluorescent nucleosides with well-characterized structural and photophysical properties. The furan-conjugated uridine **2** expands the repertoire of useful fluorescent ribonucleotides and opens new avenues for the exploration and implementation of fluorescent isosteric pyrimidine analogues.

Experimental Section

Materials. Unless otherwise specified, materials obtained from commercial suppliers were used without further purification. 5-Iodouridine was purchased from MP Biomedicals, Inc. 2-(Tributylstannyl)-furan and bis(triphenylphosphine)-palladium(II) chloride were obtained from Aldrich and Acros Chemicals, respectively. Neomycin and paromomycin were purchased as their sulfate salts from Sigma-Aldrich and were converted into free amine by passing through anion exchange resin. The identity of the aminoglycosides was established by mass measurements. DNA oligonucleotides were purchased from Integrated DNA Technologies, Inc. Oligonucleotides were purified by gel electrophoresis and desalted on a Sep-Pak (Waters Corporation). NTPs, T7 RNA polymerase, and ribonuclease inhibitor (RiboLock) were obtained from Fermentas Life Science. Custom RNA oligonucleotides procured from Dharmacon RNA Technologies were deprotected according to the supplier's procedure, gel-purified, and desalted before use. Radiolabeled α-^{32}P ATP (800 Ci/mmol) was obtained from MP Biomedicals, Inc. Alkaline phosphatase, phosphodiesterase, RNase A, and RNase T1 were purchased from Boehringer Mannheim, Germany. Chemicals for preparing buffer solutions were purchased from Fisher Biotech (enzyme grade). Autoclaved water was used in all biochemical reactions and fluorescence titrations.

Instrumentation. NMR spectra were recorded on a Varian Mercury 400 MHz spectrometer. Mass spectra were recorded at the UCSD Chemistry and Biochemistry Mass Spectrometry Facility, utilizing an LCQDECA (Finnigan) ESI with a quadrapole ion trap. All MALDI-TOF spectra were collected on a PE Biosystems Voyager-DE STR MALDI-TOF spectrometer in positive-ion, delayed-extraction mode. UV−vis spectra were recorded on a Hewlett-Packard 8452A diode array spectrometer. Reversed-phase HPLC (Vydac C18 column) purification and analysis were carried out using a Hewlett-Packard 1050 Series instrument. Steady-state fluorescence experiments were carried out in a microfluorescence cell with a path length of 1.0 cm (Hellma GmH & Co KG, Mullenheim, Germany) on a Perkin-Elmer LS 50B luminescence spectrometer. Polyacrylamide gels containing radiolabeled RNA were analyzed using a Molecular Dynamics Storm 840 phosphorimager (Amersham Pharmacia Biotech).

Synthesis. A. Furan-Modified Ribonucleoside 2. To a suspension of 5-iodouridine **1** (0.401 g, 1.08 mmol, 1 equiv) and bis(triphenylphosphine)-palladium(II) chloride (0.015 g, 0.02 mmol, 0.02 equiv) in anhydrous dioxane (20 mL) was added 2-(tributylstannyl)furan (1.746 g, 4.89 mmol, 4.5 equiv). The reaction mixture was heated at 90 °C for 2 h, cooled, and filtered through a celite bed. The solvent was evaporated, and the resulting oil was triturated with hexane (3 × 10 mL). The solid residue was redissolved in a minimum amount of hot 1:3 dichloromethane/methanol solution and was precipitated with hexane to afford the product as an off-white solid (0.33 g, 98%). ^{1}H NMR (400 MHz, d_6-DMSO): δ 11.66 (s, 1H), 8.42 (s, 1H), 7.61 (s, 1H), 6.86 (d, J = 3.2 Hz, 1H), 6.53−6.52 (m, 1H), 5.86 (d, J = 5.2 Hz, H1′, 1H), 5.43 (d, J = 5.6 Hz, OH, 1H), 5.20 (t, J = 4.6 Hz, OH, 1H), 5.11 (d, J = 5.2 Hz, OH, 1H), 4.13−4.0 (m, H2′, H3′, 2H), 3.90 (d, J = 3.2 Hz, H4′, 1H), 3.71−3.57 (m, H5′, 2H); ^{13}C NMR (100 MHz, d_6-DMSO): δ 159.84, 149.44, 146.13, 141.34, 134.69, 111.42, 107.81, 105.51, 88.06, 84.82, 73.94, 69.80, 60.54. ESI-MS (*m/z*): Calculated for $C_{13}H_{14}N_2O_7$ [M] 310.08; found $[M + 1]^+ = 310.84$, $[M + Na]^+ = 332.94$. $\lambda_{max}(H_2O) = 254$ nm (ϵ = 12 345 M^{-1} cm^{-1}), λ_{260} = 11 120 M^{-1} cm^{-1}.

B. Furan-Modified Ribonucleoside Triphosphate 2TP. To an ice cold solution of nucleoside **2** (0.044 g, 0.14 mmol, 1 equiv) in trimethyl phosphate (0.7 mL) was added freshly distilled $POCl_3$ (0.32 μL, 0.35 mmol, 2.5 equiv). The reaction mixture was stirred for 30 h at 0−4 °C. A solution of bis-tributylammonium pyrophosphate[45] (0.5 M in DMF, 1.5 mL, 0.75 mmol, 5.4 equiv) and tributyl amine (0.35 mL, 1.47 mmol, 10.5 equiv) was then rapidly added under ice-cold conditions. The reaction mixture was quenched after 15 min with 1 M triethylammonium bicarbonate buffer (TEAB, pH 7.5, 10 mL). The reaction mixture was extracted with ethyl acetate (20 mL), and the aqueous layer was evaporated under a vacuum. The residue was purified first on a DEAE sephadex-A25 anion exchange column (0.01−1.0 M, TEAB buffer, pH 7.5) followed by reversed-phase HPLC (Vydac C18 column, 1.0 cm × 25 cm, 5 μm TP silica, 0−15% acetonitrile in 100 mM triethyl ammonium acetate buffer, 30 min). Appropriate fractions were repeatedly lyophilized to afford the desired triphosphate product (0.045 g, 33%). ^{1}H NMR (400 MHz, D_2O): δ 8.25 (s, 1H), 7.63 (d, J = 0.8 Hz, 1H), 6.92 (d, J = 3.2 Hz, 1H), 6.57 (dd, J = 3.2 Hz, J = 1.6 Hz, 1H), 6.08 (d, J = 5.6 Hz, H1′, 1H), 4.54−4.48 (m, H2′, H3′, 2H), 4.36−4.28 (m, H4′, H5′, 3H); ^{13}C NMR (100 MHz, D_2O): δ 162.34, 150.89, 145.23, 142.69, 135.50, 111.50, 108.98, 107.60, 88.52, 83.80 (d, J_{PC} = 9.2 Hz), 73.78, 70.02, 65.52 (d, J_{PC} = 7.2 Hz); ^{31}P NMR (162 MHz, D_2O): −9.19 (d, J = 20.4 Hz, P_γ), −10.78 (d, J = 20.3 Hz, P_α), −22.23 (t, J = 19.8 Hz, P_β). ESI-MS (negative mode): Calculated for $C_{13}H_{17}N_2O_{16}P_3$ [M] 549.98; found $[M - H]^-$ = 548.92.

Transcription Reactions with α-^{32}P ATP. Single-strand DNA templates were annealed to an 18-mer T7 RNA polymerase consensus promoter sequence in TE buffer (10 mM Tris-HCl, 1 mM EDTA, 100 mM NaCl, pH 7.8) by heating a 1:1 mixture (5 μM) at 90 °C for 2 min and cooling the solution slowly to room temperature. Transcription reactions were performed in 40 mM Tris-HCl buffer (pH 7.9) containing 250 nM annealed template, 10 mM $MgCl_2$, 10 mM dithiothreitol (DTT), 10 mM NaCl, 2 mM spermidine, 1 U/μL RNase inhibitor (RiboLock), 1 mM GTP, 1 mM CTP, 1 mM UTP, 1 mM **2TP**, 20 μM ATP, 5 μCi α-^{32}P ATP, and 2.5 U/μL T7 RNA polymerase (Fermentas) in a total volume of 20 μL. After 3 h at 37 °C, reactions were quenched by adding 55 μL of loading buffer (7 M urea in 10 mM Tris-HCl, 100 mM EDTA, pH 8 and 0.05% bromophenol blue), heated to 75 °C for 3 min, and loaded onto an analytical 20% denaturing polyacrylamide gel. The products on the gel were analyzed using a phosphorimager. Transcription efficiencies are reported with respect to transcription in the presence of natural nucleotides (Figure 4, lanes 1, 5, 7, 9, 11, and 13). Transcription efficiencies were determined from two independent reactions, and the errors are ±10%. A large-scale transcription reaction using template **3a** was performed in a 250 μL reaction volume under similar conditions to isolate RNA for enzymatic digestion. The reaction contained 2 mM NTPs, 2 mM **2TP**, 15 mM $MgCl_2$, 300 nM template, and 500 units of T7 RNA polymerase. After incubation for 3 h at 37 °C, the precipitated magnesium pyrophosphate was removed by centrifugation. The reaction volume was reduced to half by Speed Vac, and 25 μL of loading buffer were added. The mixture was heated at 75 °C for 3 min and loaded onto a preparative 20% denaturing polyacrylamide gel. The gel was UV shadowed; appropriate bands were excised, extracted with 0.5 M ammonium acetate, and desalted on a Sep-Pak column. Concentrations of the RNA transcript were determined using absorption spectroscopy (ϵ_{260} = 92 420 M^{-1} cm^{-1}).

Synthesis of A-site ssRNA A1. An 18-mer T7 promoter sequence was annealed to a DNA template 5′ **GGTGTGACGCCTATAGT-GAGTCGTATTA** 3′, in TE buffer as before. Transcription reactions were performed under similar conditions at 37 °C in Tris-HCl buffer containing 300 nM annealed template, 2 mM ATP, 2 mM CTP, 2 mM UTP, 2 mM **2TP**, 3 mM GTP, 20 mM $MgCl_2$, and T7 RNA polymerase (500 U) in a total volume of 250 μL. After incubation for 15 h, the full length RNA transcript was isolated and purified as described above. Concentrations of the RNA transcript were determined using absorption spectroscopy (ϵ_{260} = 100 920 M^{-1} cm^{-1}).

(45) Moffatt, J. G. *Can. J. Chem.* **1964**, *42*, 599−604.

Enzymatic Digestion. Enzymatic digestion of the large-scale transcript synthesized from template **3a** was carried out according to a reported procedure.[24] Approximately 3 nmol of the transcript were digested with snake venom phosphodiesterase I, calf intestine alkaline phosphatase, and RNase A in 500 mM Tris-HCl buffer (pH 8.5, 500 mM $MgCl_2$, 1 mM EDTA) for 17 h at 37 °C. The mixture was further treated with RNase T1 for 4 h at 37 °C. The ribonucleoside mixture obtained was analyzed by reversed-phase analytical HPLC using a Vydac C18 column (0.46 cm × 25 cm, 5 μm TP silica). Mobile phase A: 100 mM triethyl ammonium acetate buffer (pH 5.5). Mobile phase B: acetonitrile. Flow rate: 1 mL/min. Gradient: 0−10% B in 20 min, 10−20% B in 5 min and 20−100% in 10 min.

Fluorescence Binding Assay. Furan-modified RNA constructs were excited at 322 nm with an excitation slit width of 15 nm and emission slit width of 20 nm, and changes in fluorescence were monitored at the emission maximum, 433 nm. A 2-AP-modified A-site model was excited at 310 nm (slit width: 5 and 10 nm), and changes in fluorescence were monitored at the emission maximum, 371 nm. For binding experiments, A-site duplexes were formed in HEPES buffer (20 mM HEPES, 100 mM NaCl, 0.5 mM EDTA, pH 7.4) by heating a 1:1 mixture at 75 °C for 5 min and cooling the solution slowly to room temperature, followed by incubating the mixture in ice. All fluorescence titrations were performed in triplicate. The standard deviation was less than ±4% in all cases.

Binding of Aminoglycosides to A-Site Duplex Models. In a typical binding experiment, the fluorescence spectrum of a 100 μL solution of HEPES buffer in the absence of RNA or aminoglycoside was recorded. This spectral blank was subtracted from all subsequent spectra within each titration. Following determination of the buffer blank, 25 μL of either furan- or 2-AP-modifed A-site duplex (20 μM) were added (final duplex concentration, 4.0 μM). The solution was mixed well, and the spectrum was recorded again. Subsequent aliquots (1 μL) of increasing concentrations of an aminoglycoside were added, and the fluorescence spectrum was recorded after each aliquot until fluorescence saturation was achieved. EC_{50} values were calculated using KaleidaGraph software by fitting a dose response curve (eq 1) to the fractional fluorescence saturation (F_s) plotted against the log of aminoglycoside (AG) concentration.[9]

$$F_s = \frac{F_i - F_0}{F_\infty - F_0}$$

F_i is the fluorescence intensity at each titration point. F_0 and F_∞ are the fluorescence intensity in the absence of aminoglycoside or at saturation, respectively. n is the Hill coefficient or degree of cooperativity associated with the binding

$$F_s = F_0 + \left(\frac{F_\infty [\mathrm{AG}]^n}{[\mathrm{EC}_{50}]^n + [\mathrm{AG}]^n} \right) \quad (1)$$

Acknowledgment. We thank professors Daniel Pilch and Thomas Hermann for useful discussions and Mr. Nicholas Greco for help with the mass spectra measurements. We are grateful to the National Institutes of Health (GM 069773 and AI 47673) for support.

Supporting Information Available: Additional absorption and emission spectra of the nucleoside, nucleotide, and oligonucleotides; steady-state Stern−Volmer titrations of nucleoside **2**; procedures and data for mass spectral analysis of oligonucleotides; thermal denaturation studies; RNA secondary structures; and additional fluorescence titrations. This material is available free of charge via the Internet at http://pubs.acs.org.

JA066455R